

Finite Mixtures of Skewed Matrix Variate Distributions

Michael P.B. Gallagher and Paul D. McNicholas

Dept. of Mathematics & Statistics, McMaster University, Hamilton, Ontario, Canada.

Abstract

Clustering is the process of finding underlying group structures in data. Although mixture model-based clustering is firmly established in the multivariate case, there is a relative paucity of work on matrix variate distributions and none for clustering with mixtures of skewed matrix variate distributions. Four finite mixtures of skewed matrix variate distributions are considered. Parameter estimation is carried out using an expectation-conditional maximization algorithm, and both simulated and real data are used for illustration.

Keywords: Clustering; matrix variate; mixture models; skewed distributions.

1 Introduction

Over the years, there has been increased interest in the applications involving three-way (matrix variate) data. Although there are countless examples of clustering for multivariate distributions using finite mixture models, as discussed in Section 2, there is very little work for matrix variate distributions. Moreover, the examples in the literature deal exclusively with symmetric (non-skewed) matrix variate distributions such as the matrix variate normal and the matrix variate t distributions.

There are many different areas of application for matrix variate distributions. One area is multivariate longitudinal data, where multiple variables are measured over time (e.g., Anderlucci & Viroli 2015). In this case, each row of a matrix would correspond to a time point and the columns would represent each of the variables. Furthermore, the two scale matrices, a defining characteristic of matrix variate distributions, allow for simultaneous modelling of the inter-variable covariances as well as the temporal covariances. A second application, considered herein, is image recognition. In this case, an image is analyzed as an $n \times p$ pixel intensity matrix. Herein, a finite mixture of four different skewed matrix distributions, the matrix variate skew- t , generalized hyperbolic, variance-gamma and normal inverse Gaussian (NIG) distributions are considered. These mixture models are illustrated for both clustering (unsupervised classification) and semi-supervised classification using both simulated and real data.

2 Background

2.1 Model-Based Clustering and Mixture Models

Clustering and classification look at finding and analyzing underlying group structures in data. One common method used for clustering is model-based, and generally makes use of a G -component finite mixture model. A multivariate random variable \mathbf{X} from a finite mixture model has density

$$f(\mathbf{x} \mid \boldsymbol{\vartheta}) = \sum_{g=1}^G \pi_g f_g(\mathbf{x} \mid \boldsymbol{\theta}_g),$$

where $\boldsymbol{\vartheta} = (\pi_1, \pi_2, \dots, \pi_G, \boldsymbol{\theta}_1, \boldsymbol{\theta}_2, \dots, \boldsymbol{\theta}_G)$, $f_g(\cdot)$ is the g th component density, and $\pi_g > 0$ is the g th mixing proportion such that $\sum_{i=1}^G \pi_g = 1$. McNicholas (2016a) traces the association between clustering and mixture models back to Tiedeman (1955), and the earliest use of a finite mixture model for clustering can be found in Wolfe (1965), who uses a Gaussian mixture model. Other early work in this area can be found in Baum, Petrie, Soules & Weiss (1970) and Scott & Symons (1971), and a recent review of model-based clustering is given by McNicholas (2016b).

Although the Gaussian mixture model is well-established for clustering, largely due to its mathematical tractability, quite some work has been done in the area of non-Gaussian mixtures. For example, some work has been done using symmetric component densities that parameterize concentration (tail weight), e.g., the t distribution (Peel & McLachlan 2000, Andrews & McNicholas 2011, 2012, Lin, McNicholas & Hsiu 2014) and the power exponential distribution (Dang, Browne & McNicholas 2015). There has also been work on mixtures for discrete data (e.g., Karlis & Meligkotsidou 2007, Bouguila & ElGuebaly 2009) as well as several examples of mixtures of skewed distributions such as the NIG distribution (Karlis & Santourian 2009, Subedi & McNicholas 2014), the skew- t distribution (Lin 2010, Vrbik & McNicholas 2012, 2014, Murray, McNicholas & Browne 2014, Lee & McLachlan 2014, 2016, Murray, Browne & McNicholas 2014, 2017), the shifted asymmetric Laplace distribution (Morris & McNicholas 2013, Franczak, Browne & McNicholas 2014), the variance-gamma distribution (McNicholas, McNicholas & Browne 2017), the generalized hyperbolic distribution (Browne & McNicholas 2015), and others (e.g., Elguebaly & Bouguila 2015, Franczak, Tortora, Browne & McNicholas 2015).

Recently, there has been an interest in the mixtures of matrix variate distributions, e.g., Anderlucci & Viroli (2015) consider multivariate longitudinal data with the matrix variate normal distribution and Doğru, Bulut & Arslan (2016) consider a finite mixture of matrix variate t distributions.

2.2 Matrix Variate Distributions

Three-way data such as multivariate longitudinal data or greyscale image data can be easily modelled using a matrix variate distribution. There are many examples of such distributions

presented in the literature, the most notable being the matrix variate normal distribution. In Section 2.1, \mathbf{X} was used in the typical way to denote a multivariate random variable and \mathbf{x} was used to denote its realization. Hereafter, \mathbf{X} is used to denote a realization of a random matrix \mathcal{X} . An $n \times p$ random matrix \mathcal{X} follows an $n \times p$ matrix variate normal distribution with location parameter \mathbf{M} and scale matrices $\mathbf{\Sigma}$ and $\mathbf{\Psi}$ of dimensions $n \times n$ and $p \times p$, respectively, denoted by $\mathcal{N}_{n \times p}(\mathbf{M}, \mathbf{\Sigma}, \mathbf{\Psi})$ if the density of \mathcal{X} can be written as

$$f(\mathbf{X} \mid \mathbf{M}, \mathbf{\Sigma}, \mathbf{\Psi}) = \frac{1}{(2\pi)^{\frac{np}{2}} |\mathbf{\Sigma}|^{\frac{p}{2}} |\mathbf{\Psi}|^{\frac{n}{2}}} \exp \left\{ -\frac{1}{2} \text{tr} (\mathbf{\Sigma}^{-1}(\mathbf{X} - \mathbf{M})\mathbf{\Psi}^{-1}(\mathbf{X} - \mathbf{M})') \right\}. \quad (1)$$

A well known property of the matrix variate normal distribution (Harrar & Gupta 2008) is

$$\mathcal{X} \sim \mathcal{N}_{n \times p}(\mathbf{M}, \mathbf{\Sigma}, \mathbf{\Psi}) \iff \text{vec}(\mathcal{X}) \sim \mathcal{N}_{np}(\text{vec}(\mathbf{M}), \mathbf{\Psi} \otimes \mathbf{\Sigma}), \quad (2)$$

where $\mathcal{N}_{np}(\cdot)$ is the multivariate normal density with dimension np , $\text{vec}(\cdot)$ is the vectorization operator, and \otimes is the Kronecker product.

The matrix variate normal distribution has many elegant mathematical properties that have made it so popular, e.g., Viroli (2011) uses a mixture of matrix variate normal distributions for clustering. However, there are non-normal examples such as the Wishart distribution (Wishart 1928) and the skew-normal distribution, e.g., Chen & Gupta (2005), Domínguez-Molina, González-Farías, Ramos-Quiroga & Gupta (2007), and Harrar & Gupta (2008). More information on matrix variate distributions can be found in Gupta & Nagar (1999).

2.3 The Generalized Inverse Gaussian Distribution

The generalized inverse Gaussian distribution has two different parameterizations, both of which will be useful. A random variable Y has a generalized inverse Gaussian (GIG) distribution parameterized by a, b and λ , denoted by $\text{GIG}(a, b, \lambda)$, if its probability density function can be written as

$$f(y|a, b, \lambda) = \frac{(a/b)^{\frac{\lambda}{2}} y^{\lambda-1}}{2K_{\lambda}(\sqrt{ab})} \exp \left\{ -\frac{ay + b/y}{2} \right\},$$

where

$$K_{\lambda}(u) = \frac{1}{2} \int_0^{\infty} y^{\lambda-1} \exp \left\{ -\frac{u}{2} \left(y + \frac{1}{y} \right) \right\} dy$$

is the modified Bessel function of the third kind with index λ . Expectations of some functions of a GIG random variable have a mathematically tractable form, e.g.:

$$\mathbb{E}(Y) = \sqrt{\frac{b}{a}} \frac{K_{\lambda+1}(\sqrt{ab})}{K_{\lambda}(\sqrt{ab})}, \quad (3)$$

$$\mathbb{E}(1/Y) = \sqrt{\frac{a}{b}} \frac{K_{\lambda+1}(\sqrt{ab})}{K_{\lambda}(\sqrt{ab})} - \frac{2\lambda}{b}, \quad (4)$$

$$\mathbb{E}(\log Y) = \log \left(\sqrt{\frac{b}{a}} \right) + \frac{1}{K_{\lambda}(\sqrt{ab})} \frac{\partial}{\partial \lambda} K_{\lambda}(\sqrt{ab}). \quad (5)$$

Although this parameterization of the GIG distribution will be useful for parameter estimation, for the purposes of deriving the density of the matrix variate generalized hyperbolic distribution, it is more useful to take the parameterization

$$g(y|\omega, \eta, \lambda) = \frac{(w/\eta)^{\lambda-1}}{2\eta K_{\lambda}(\omega)} \exp \left\{ -\frac{\omega}{2} \left(\frac{w}{\eta} + \frac{\eta}{w} \right) \right\}, \quad (6)$$

where $\omega = \sqrt{ab}$ and $\eta = \sqrt{a/b}$. For notational clarity, we will denote the parameterization given in (6) by $I(\omega, \eta, \lambda)$.

2.4 Skewed Matrix Variate Distributions

The work of Gallaugher & McNicholas (2017*a,b*) presents a total of four skewed matrix variate distributions, the matrix variate skew- t , generalized hyperbolic, variance-gamma and NIG distributions. Each of these distributions is derived from a matrix variate normal variance-mean mixture. In this representation, the random matrix \mathcal{X} has the representation

$$\mathcal{X} = \mathbf{M} + W\mathbf{A} + \sqrt{W}\mathcal{V}, \quad (7)$$

where \mathbf{M} and \mathbf{A} are $n \times p$ matrices representing the location and skewness respectively, $\mathcal{V} \sim \mathcal{N}_{n \times p}(\mathbf{0}, \Sigma, \Psi)$, and $W > 0$ is a random variable with density $h(w|\boldsymbol{\theta})$.

In Gallaugher & McNicholas (2017*a*), the matrix variate skew- t distribution, with ν degrees of freedom, is shown to arise as a special case of (7) with $W^{\text{ST}} \sim \text{IGamma}(\nu/2, \nu/2)$, where $\text{IGamma}(\cdot)$ denotes the inverse Gamma distribution with density

$$f(y | a, b) = \frac{b^a}{\Gamma(a)} y^{-a-1} \exp \left\{ -\frac{b}{y} \right\}.$$

The resulting density of \mathcal{X} is

$$f_{\text{MVST}}(\mathbf{X} | \boldsymbol{\theta}) = \frac{2 \left(\frac{\nu}{2} \right)^{\frac{\nu}{2}} \exp \{ \text{tr}(\Sigma^{-1}(\mathbf{X} - \mathbf{M})\Psi^{-1}\mathbf{A}') \}}{(2\pi)^{\frac{np}{2}} |\Sigma|^{\frac{p}{2}} |\Psi|^{\frac{n}{2}} \Gamma(\frac{\nu}{2})} \left(\frac{\delta(\mathbf{X}; \mathbf{M}, \Sigma, \Psi) + \nu}{\rho(\mathbf{A}, \Sigma, \Psi)} \right)^{-\frac{\nu+np}{4}} \\ \times K_{-\frac{\nu+np}{2}} \left(\sqrt{[\rho(\mathbf{A}, \Sigma, \Psi)] [\delta(\mathbf{X}; \mathbf{M}, \Sigma, \Psi) + \nu]} \right),$$

where

$$\delta(\mathbf{X}; \mathbf{M}, \Sigma, \Psi) = \text{tr}(\Sigma^{-1}(\mathbf{X} - \mathbf{M})\Psi^{-1}(\mathbf{X} - \mathbf{M}')), \quad \rho(\mathbf{A}; \Sigma, \Psi) = \text{tr}(\Sigma^{-1}\mathbf{A}\Psi^{-1}\mathbf{A}')$$

and $\nu > 0$. For notational clarity, this distribution will be denoted by $\text{MVST}(\mathbf{M}, \mathbf{A}, \mathbf{\Sigma}, \mathbf{\Psi}, \nu)$.

In Gallaugher & McNicholas (2017b), one of the distributions considered is a matrix variate generalized hyperbolic distribution. This again is the result of a special case of (7) with $W^{\text{GH}} \sim \text{I}(\omega, 1, \lambda)$. This distribution will be denoted by $\text{MVGH}(\mathbf{M}, \mathbf{A}, \mathbf{\Sigma}, \mathbf{\Psi}, \lambda, \omega)$, and the density is

$$f_{\text{MVGH}}(\mathbf{X}|\boldsymbol{\vartheta}) = \frac{\exp\{\text{tr}(\mathbf{\Sigma}^{-1}(\mathbf{X} - \mathbf{M})\mathbf{\Psi}^{-1}\mathbf{A}')\}}{(2\pi)^{\frac{np}{2}}|\mathbf{\Sigma}|^{\frac{p}{2}}|\mathbf{\Psi}|^{\frac{n}{2}}K_{\lambda}(\omega)} \left(\frac{\delta(\mathbf{X}; \mathbf{M}, \mathbf{\Sigma}, \mathbf{\Psi}) + \omega}{\rho(\mathbf{A}, \mathbf{\Sigma}, \mathbf{\Psi}) + \omega} \right)^{\frac{(\lambda - \frac{np}{2})}{2}} \\ \times K_{(\lambda - np/2)} \left(\sqrt{[\rho(\mathbf{A}, \mathbf{\Sigma}, \mathbf{\Psi}) + \omega][\delta(\mathbf{X}; \mathbf{M}, \mathbf{\Sigma}, \mathbf{\Psi}) + \omega]} \right),$$

where $\lambda \in \mathbb{R}$ and $\omega > 0$.

The matrix variate variance-gamma distribution, also derived in Gallaugher & McNicholas (2017b), denoted $\text{MVVG}(\mathbf{M}, \mathbf{A}, \mathbf{\Sigma}, \mathbf{\Psi}, \gamma)$ is a special case of the matrix variate normal variance-mean mixture (7) with $W^{\text{VG}} \sim \text{gamma}(\gamma, \gamma)$, where $\text{gamma}(\cdot)$ denotes the gamma distribution with density

$$f(y | a, b) = \frac{b^a}{\Gamma(a)} y^{a-1} \exp\{-by\}.$$

The density of the random matrix \mathcal{X} with this distribution is

$$f_{\text{MVVG}}(\mathbf{X}|\boldsymbol{\vartheta}) = \frac{2\gamma^{\gamma} \exp\{\text{tr}(\mathbf{\Sigma}^{-1}(\mathbf{X} - \mathbf{M})\mathbf{\Psi}^{-1}\mathbf{A}')\}}{(2\pi)^{\frac{np}{2}}|\mathbf{\Sigma}|^{\frac{p}{2}}|\mathbf{\Psi}|^{\frac{n}{2}}\Gamma(\gamma)} \left(\frac{\delta(\mathbf{X}; \mathbf{M}, \mathbf{\Sigma}, \mathbf{\Psi})}{\rho(\mathbf{A}, \mathbf{\Sigma}, \mathbf{\Psi}) + 2\gamma} \right)^{\frac{(\gamma - np/2)}{2}} \\ \times K_{(\gamma - \frac{np}{2})} \left(\sqrt{[\rho(\mathbf{A}, \mathbf{\Sigma}, \mathbf{\Psi}) + 2\gamma][\delta(\mathbf{X}; \mathbf{M}, \mathbf{\Sigma}, \mathbf{\Psi})]} \right),$$

where $\gamma > 0$.

Finally, the matrix variate NIG distribution arises when $W^{\text{NIG}} \sim \text{IG}(1, \tilde{\gamma})$, where $\text{IG}(\cdot)$ denotes the inverse-Gaussian distribution with density

$$f(y | \delta, \gamma) = \frac{\delta}{\sqrt{2\pi}} \exp\{\delta\gamma\} y^{-\frac{3}{2}} \exp\left\{-\frac{1}{2}\left(\frac{\delta^2}{y} + \gamma^2 y\right)\right\}.$$

The density of \mathcal{X} is

$$f_{\text{MVNIG}}(\mathbf{X}|\boldsymbol{\vartheta}) = \frac{2 \exp\{\text{tr}(\mathbf{\Sigma}^{-1}(\mathbf{X} - \mathbf{M})\mathbf{\Psi}^{-1}\mathbf{A}') + \tilde{\gamma}\}}{(2\pi)^{\frac{np+1}{2}}|\mathbf{\Sigma}|^{\frac{p}{2}}|\mathbf{\Psi}|^{\frac{n}{2}}} \left(\frac{\delta(\mathbf{X}; \mathbf{M}, \mathbf{\Sigma}, \mathbf{\Psi}) + 1}{\rho(\mathbf{A}, \mathbf{\Sigma}, \mathbf{\Psi}) + \tilde{\gamma}^2} \right)^{-(1+np)/4} \\ \times K_{-(1+np)/2} \left(\sqrt{[\rho(\mathbf{A}, \mathbf{\Sigma}, \mathbf{\Psi}) + \tilde{\gamma}^2][\delta(\mathbf{X}; \mathbf{M}, \mathbf{\Sigma}, \mathbf{\Psi}) + 1]} \right),$$

where $\tilde{\gamma} > 0$. This distribution is denoted by $\text{MVNIG}(\mathbf{M}, \mathbf{A}, \mathbf{\Sigma}, \mathbf{\Psi}, \tilde{\gamma})$.

2.5 Benefits Over Vectorization

One alternative to matrix variate analysis for matrix variate data is to consider the vectorization of the data and perform multivariate techniques. However, the benefits of using matrix variate methods are twofold. The first being specifically for the case of multivariate longitudinal data. Performing the analysis using a matrix variate model has the benefit of simultaneously considering the temporal covariances (via Σ) as well as the covariances for the variables (via Ψ). Performing multivariate analysis on the vectorization of the data would not have this benefit without imposing some structure on the scale matrix.

The second benefit is the reduction in the number of parameters. If the matrix variate data is $n \times p$, vectorization would result in np dimensional vectors, therefore resulting in $(n^2p^2 + np)/2$ free scale parameters when using multivariate analysis. However, when using a matrix variate model, there are two lower dimensional matrices that comprise the scale parameters with a total of $(n^2 + p^2 + n + p)/2$ free scale parameters. Thus, for $n = p$, there is a reduction from quartic to quadratic complexity in n and, for almost all values of n and p , there will be a (often substantial) reduction in the number of free scale parameters.

3 Methodology

3.1 Likelihoods

In the mixture model context, \mathcal{X} is assumed to come from a population with G subgroups each distributed according to the same one of the four skewed matrix variate distributions discussed previously. Now suppose N $n \times p$ matrices $\mathbf{X}_1, \mathbf{X}_2, \dots, \mathbf{X}_N$ are observed, then the observed-data likelihood is

$$L(\boldsymbol{\vartheta}) = \prod_{i=1}^N \sum_{g=1}^G \pi_g f(\mathbf{X}_i \mid \mathbf{M}_g, \mathbf{A}_g, \Sigma_g, \Psi_g, \boldsymbol{\theta}_g),$$

where $\boldsymbol{\theta}_g$ are the parameters associated with the distribution of W_{ig} . For the purposes of parameter estimation, we proceed as if the observed data is incomplete. In particular, we introduce the missing group membership indicators z_{ig} , where

$$z_{ig} = \begin{cases} 1 & \text{if } \mathbf{X}_i \text{ is in group } g, \\ 0 & \text{otherwise.} \end{cases}$$

In addition to the missing z_{ig} , we also have the latent variables W_{ig} and we denote their densities by $h(w_{ig} \mid \boldsymbol{\theta}_g)$.

The complete-data log-likelihood, in its general form for any of the distributions already discussed, is then

$$\ell_c(\boldsymbol{\vartheta}) = \mathcal{L}_1 + (\mathcal{L}_2 + C_2) + (\mathcal{L}_3 + C_3), \quad (8)$$

where C_2 and C_3 are constant with respect to the parameters, $\mathcal{L}_1 = \sum_{i=1}^N \sum_{g=1}^G z_{ig} \pi_g$, $\mathcal{L}_2 = \sum_{i=1}^N \sum_{g=1}^G z_{ig} h(w_{ig} \mid \boldsymbol{\theta}_g) - C_2$, and

$$\mathcal{L}_3 = \frac{1}{2} \sum_{i=1}^N \sum_{g=1}^G z_{ig} \left[\text{tr}(\boldsymbol{\Sigma}_g^{-1}(\mathbf{X}_i - \mathbf{M}_g)\boldsymbol{\Psi}_g^{-1}\mathbf{A}_g') + \text{tr}(\boldsymbol{\Sigma}_g^{-1}\mathbf{A}_g\boldsymbol{\Psi}_g^{-1}(\mathbf{X}_i - \mathbf{M}_g)') \right. \\ \left. - \frac{1}{w_{ig}} \text{tr}(\boldsymbol{\Sigma}_g^{-1}(\mathbf{X}_i - \mathbf{M}_g)\boldsymbol{\Psi}_g^{-1}(\mathbf{X}_i - \mathbf{M}_g)') - w_{ig} \text{tr}(\boldsymbol{\Sigma}_g^{-1}\mathbf{A}_g\boldsymbol{\Psi}_g^{-1}\mathbf{A}_g') - p \log(|\boldsymbol{\Sigma}_g|) - n \log(|\boldsymbol{\Psi}_g|) \right].$$

3.2 Parameter Estimation

Parameter estimation is performed by using an expectation-conditional maximization (ECM) algorithm (Meng & Rubin 1993).

1) Initialization: Initialize the parameters $\mathbf{M}_g, \mathbf{A}_g, \boldsymbol{\Sigma}_g, \boldsymbol{\Psi}_g$ and other parameters related to the distribution. Set $t = 0$.

2) E Step: Update $\hat{z}_{ig}, a_{ig}, b_{ig}, c_{ig}$, where

$$\hat{z}_{ig}^{(t+1)} = \frac{\pi_g f(\mathbf{X}_i \mid \hat{\boldsymbol{\theta}}_g^{(t)})}{\sum_{h=1}^G \pi_h f(\mathbf{X}_i \mid \hat{\boldsymbol{\theta}}_h^{(t)})}, \quad a_{ig}^{(t+1)} = \mathbb{E}(W_{ig} \mid \mathbf{X}_i, z_{ig} = 1, \hat{\boldsymbol{\theta}}_g^{(t)}), \\ b_{ig}^{(t+1)} = \mathbb{E}\left(\frac{1}{W_{ig}} \mid \mathbf{X}_i, z_{ig} = 1, \hat{\boldsymbol{\theta}}_g^{(t)}\right), \quad c_{ig}^{(t+1)} = \mathbb{E}(\log(W_{ig}) \mid \mathbf{X}_i, z_{ig} = 1, \hat{\boldsymbol{\theta}}_g^{(t)}).$$

Note that the specific updates will depend on the distribution. However, in each case, the conditional distribution of W_{ig} given the observed data and group memberships is a generalized inverse Gaussian distribution. Specifically,

$$W_{ig}^{\text{ST}} \mid \mathbf{X}_i, z_{ig} = 1 \sim \text{GIG}(\rho(\mathbf{A}_g, \boldsymbol{\Sigma}_g, \boldsymbol{\Psi}_g), \delta(\mathbf{X}; \mathbf{M}_g, \boldsymbol{\Sigma}_g, \boldsymbol{\Psi}_g) + \nu_g, -(\nu_g + np)/2), \\ W_{ig}^{\text{GH}} \mid \mathbf{X}_i, z_{ig} = 1 \sim \text{GIG}(\rho(\mathbf{A}_g, \boldsymbol{\Sigma}_g, \boldsymbol{\Psi}_g) + \omega_g, \delta(\mathbf{X}; \mathbf{M}_g, \boldsymbol{\Sigma}_g, \boldsymbol{\Psi}_g) + \omega_g, \lambda_g - np/2), \\ W_{ig}^{\text{VG}} \mid \mathbf{X}_i, z_{ig} = 1 \sim \text{GIG}(\rho(\mathbf{A}_g, \boldsymbol{\Sigma}_g, \boldsymbol{\Psi}_g) + 2\gamma_g, \delta(\mathbf{X}; \mathbf{M}_g, \boldsymbol{\Sigma}_g, \boldsymbol{\Psi}_g), \gamma_g - np/2), \\ W_{ig}^{\text{NIG}} \mid \mathbf{X}_i, z_{ig} = 1 \sim \text{GIG}(\rho(\mathbf{A}_g, \boldsymbol{\Sigma}_g, \boldsymbol{\Psi}_g) + \tilde{\gamma}_g^2, \delta(\mathbf{X}; \mathbf{M}_g, \boldsymbol{\Sigma}_g, \boldsymbol{\Psi}_g) + 1, -(1 + np)/2).$$

Therefore, the exact updates are obtained by using the expectations given in (3)–(5) for appropriate values of λ, a , and b .

3) First CM Step: Update the parameters $\pi_g, \mathbf{M}_g, \mathbf{A}_g$.

$$\hat{\pi}_g^{(t+1)} = \frac{N_g}{N}, \quad \hat{\mathbf{M}}_g^{(t+1)} = \frac{\sum_{i=1}^N \hat{z}_{ig}^{(t+1)} \mathbf{X}_i (\bar{a}_g^{(t+1)} b_{ig}^{(t+1)} - 1)}{\sum_{i=1}^N \hat{z}_{ig}^{(t+1)} \bar{a}_g^{(t+1)} b_{ig}^{(t+1)} - N_g}, \\ \hat{\mathbf{A}}_g^{(t+1)} = \frac{\sum_{i=1}^N \hat{z}_{ig}^{(t+1)} \mathbf{X}_i (\bar{b}_g^{(t+1)} - b_{ig}^{(t+1)})}{\sum_{i=1}^N \hat{z}_{ig}^{(t+1)} \bar{a}_g^{(t+1)} b_{ig}^{(t+1)} - N_g},$$

where

$$N_g = \sum_{i=1}^N \hat{z}_{ig}^{(t+1)}, \quad \bar{a}_g^{(t+1)} = \frac{\sum_{i=1}^N \hat{z}_{ig}^{(t+1)} a_{ig}^{(t+1)}}{N_g}, \quad \bar{b}_g^{(t+1)} = \frac{\sum_{i=1}^N \hat{z}_{ig}^{(t+1)} b_{ig}^{(t+1)}}{N_g}.$$

4) Second CM Step: Update Σ_g

$$\begin{aligned} \hat{\Sigma}_g^{(t+1)} = \frac{1}{N_g p} & \left[\sum_{i=1}^N \hat{z}_{ig}^{(t+1)} \left(b_{ig}^{(t+1)} \left(\mathbf{X}_i - \hat{\mathbf{M}}_g^{(t+1)} \right) \hat{\Psi}_g^{(t)}{}^{-1} \left(\mathbf{X}_i - \hat{\mathbf{M}}_g^{(t+1)} \right)' \right. \right. \\ & - \hat{\mathbf{A}}_g^{(t+1)} \hat{\Psi}_g^{(t)}{}^{-1} \left(\mathbf{X}_i - \hat{\mathbf{M}}_g^{(t+1)} \right)' - \left(\mathbf{X}_i - \hat{\mathbf{M}}_g^{(t+1)} \right) \hat{\Psi}_g^{(t)}{}^{-1} \hat{\mathbf{A}}_g^{(t+1)}' \\ & \left. \left. + a_{ig}^{(t+1)} \hat{\mathbf{A}}_g^{(t+1)} \hat{\Psi}_g^{(t)}{}^{-1} \hat{\mathbf{A}}_g^{(t+1)}' \right) \right]. \end{aligned} \quad (9)$$

5) Third CM Step: Update Ψ_g

$$\begin{aligned} \hat{\Psi}_g^{(t+1)} = \frac{1}{N_g n} & \left[\sum_{i=1}^N \hat{z}_{ig}^{(t+1)} \left(b_{ig}^{(t+1)} \left(\mathbf{X}_i - \hat{\mathbf{M}}_g^{(t+1)} \right)' \hat{\Sigma}_g^{(t+1)}{}^{-1} \left(\mathbf{X}_i - \hat{\mathbf{M}}_g^{(t+1)} \right) \right. \right. \\ & - \hat{\mathbf{A}}_g^{(t+1)}' \hat{\Sigma}_g^{(t+1)}{}^{-1} \left(\mathbf{X}_i - \hat{\mathbf{M}}_g^{(t+1)} \right) - \left(\mathbf{X}_i - \hat{\mathbf{M}}_g^{(t+1)} \right)' \hat{\Sigma}_g^{(t+1)}{}^{-1} \hat{\mathbf{A}}_g^{(t+1)} \\ & \left. \left. + a_{ig}^{(t+1)} \hat{\mathbf{A}}_g^{(t+1)}' \hat{\Sigma}_g^{(t+1)}{}^{-1} \hat{\mathbf{A}}_g^{(t+1)} \right) \right]. \end{aligned} \quad (10)$$

6) Other CM Steps: The additional parameters introduced by the distribution of W_{ig} are now updated. These updates will vary according the distribution and the particulars for the MVST, MVGH, MVVG and MVNIG distributions are given below.

7) Check Convergence: If not converged, set $t = t + 1$ and return to step 2).

Matrix Variate Skew- t Distribution

In the case of the matrix variate skew- t distribution, the degrees of freedom ν_g need to be updated. This update cannot be obtained in closed form, and thus needs to be performed numerically. We have

$$\mathcal{L}_2^{\text{MVST}} = \sum_{i=1}^N \sum_{g=1}^G z_{ig} \left[\frac{\nu_g}{2} \log \left(\frac{\nu_g}{2} \right) - \log \left(\Gamma \left(\frac{\nu_g}{2} \right) \right) - \frac{\nu_g}{2} \left(\log(w_{ig}) + \frac{1}{w_{ig}} \right) \right].$$

Therefore, the update $\nu_g^{(t+1)}$ is obtained by solving (11) for ν_g , i.e.,

$$\log \left(\frac{\nu_g}{2} \right) + 1 - \varphi \left(\frac{\nu_g}{2} \right) - \frac{1}{N_g} \sum_{i=1}^N \hat{z}_{ig}^{(t+1)} (b_{ig}^{(t+1)} + c_{ig}^{(t+1)}) = 0, \quad (11)$$

where $\varphi(\cdot)$ denotes the digamma function.

Matrix Variate Generalized Hyperbolic Distribution

In the case of the matrix variate generalized hyperbolic distribution, updates for λ_g and ω_g are needed. In this case,

$$\mathcal{L}_2^{\text{MVGH}} = \sum_{i=1}^N \sum_{g=1}^G z_{ig} \left[\log(K_{\lambda_g}(\omega_g)) - \lambda_g \log w_{ig} - \frac{1}{2} \omega_g \left(w_{ig} + \frac{1}{w_{ig}} \right) \right]. \quad (12)$$

The updates for λ_g and ω_g cannot be obtained in closed form. However, Browne & McNicholas (2015) discuss numerical methods for these updates and, because the portion of the likelihood function that include these parameters is the same as in the multivariate case, the updates described in Browne & McNicholas (2015) can be used directly here.

The updates for λ_g and ω_g rely on the log-convexity of $K_s(t)$ in both s and t (Baricz 2010) and maximizing (12) via conditional maximization. The resulting updates are

$$\hat{\lambda}_g^{(t+1)} = \bar{c}_g^{(t+1)} \hat{\lambda}_g^{(t)} \left[\frac{\partial}{\partial s} \log(K_s(\hat{\omega}_g^{(t)})) \Big|_{s=\hat{\lambda}_g^{(t)}} \right]^{-1}, \quad (13)$$

$$\hat{\omega}_g^{(t+1)} = \hat{\omega}_g^{(t)} - \left[\frac{\partial}{\partial s} q(\hat{\lambda}_g^{(t+1)}, s) \Big|_{s=\hat{\omega}_g^{(t)}} \right] \left[\frac{\partial^2}{\partial s^2} q(\hat{\lambda}_g^{(t+1)}, s) \Big|_{s=\hat{\omega}_g^{(t)}} \right]^{-1}, \quad (14)$$

where the derivative in (13) is calculated numerically,

$$q(\lambda_g, \omega_g) = \sum_{i=1}^N z_{ig} \left[\log(K_{\lambda_g}(\omega_g)) - \lambda_g \log w_{ig} - \frac{1}{2} \omega_g \left(w_{ig} + \frac{1}{w_{ig}} \right) \right]$$

and $\bar{c}_g^{(t+1)} = (1/N_g) \sum_{i=1}^N \hat{z}_{ig}^{(t+1)} c_{ig}^{(t+1)}$. The partials in (14) are described in Browne & McNicholas (2015) and can be written as

$$\frac{\partial}{\partial \omega_g} q(\lambda_g, \omega_g) = \frac{1}{2} [R_{\lambda_g}(\omega_g) + R_{-\lambda_g}(\omega_g) - (\bar{a}_g^{(t+1)} + \bar{b}_g^{(t+1)})],$$

and

$$\frac{\partial^2}{\partial \omega_g^2} q(\lambda_g, \omega_g) = \frac{1}{2} \left[R_{\lambda_g}(\omega_g)^2 - \frac{1 + 2\lambda_g}{\omega_g} R_{\lambda_g}(\omega_g) - 1 + R_{-\lambda_g}(\omega_g)^2 - \frac{1 - 2\lambda_g}{\omega_g} R_{-\lambda_g}(\omega_g) - 1 \right],$$

where $R_{\lambda_g}(\omega_g) = K_{\lambda_g+1}(\omega_g)/K_{\lambda_g}(\omega_g)$.

Matrix Variate Variance-Gamma Distribution

In the case of the matrix variate variance-gamma,

$$\mathcal{L}_2^{\text{MVVG}} = \sum_{i=1}^N \sum_{g=1}^G z_{ig} [\gamma_g \log \gamma_g - \log \Gamma(\gamma_g) + \gamma_g (\log w_{ig} - w_{ig})].$$

The update for γ_g , as in the skew-t case, cannot be obtained in closed form. Instead, the update $\gamma_g^{(t+1)}$ is obtained by solving (15) for γ_g , where

$$\log \gamma_g + 1 - \varphi(\gamma_g) + \bar{c}_g^{(t+1)} - \bar{a}_g^{(t+1)} = 0. \quad (15)$$

Matrix Variate NIG Distribution

In this case, $\tilde{\gamma}_g$ needs to be updated. Note that

$$\mathcal{L}_2^{\text{MVNIG}} = \sum_{i=1}^N \sum_{g=1}^G z_{ig} \tilde{\gamma}_g - \frac{\tilde{\gamma}_g^2}{2} z_{ig} w_{ig}$$

and, therefore, the closed form updates for $\tilde{\gamma}_g$ are

$$\tilde{\gamma}_g^{(t+1)} = \frac{N_g}{\bar{a}_g^{(t+1)}}.$$

3.3 Numerical Considerations and Convergence Criterion

The main numerical problem encountered is the calculation of the Bessel function $K_\lambda(x)$ and the calculation of its partial derivative with respect to λ . When x becomes large relative to λ , the Bessel function is rounded to zero. One solution is to consider the evaluation of $\exp\{x\}K_\lambda(x)$ and then make adjustments to subsequent calculations. In most of the simulations (Section 4), this helped with the evaluation of the densities and the numerical derivatives. However, for the real data application (Section 5), the issue is that $|\lambda|$ becomes too large due to the dimension and the Bessel function tends to infinity. This is an indication that dimension reduction techniques will need to be considered in the future (see Section 6).

There are several options for determining convergence of this ECM algorithm. The criterion used in the simulations in Section 4 is based on the Aitken acceleration Aitken (1926). The Aitken acceleration at iteration t is

$$a^{(t)} = \frac{l^{(t+1)} - l^{(t)}}{l^{(t)} - l^{(t-1)}},$$

where $l^{(t)}$ is the (observed) log-likelihood at iteration t . We then define

$$l_\infty^{(t+1)} = l^{(t)} + \frac{1}{1 - a^{(t)}}(l^{(t+1)} - l^{(t)})$$

(see Böhning, Dietz, Schaub, Schlattmann & Lindsay 1994, Lindsay 1995). The quantity l_∞ is an asymptotic estimate (i.e., an estimate of the value after many iterations) of the log-likelihood at iteration $t+1$. As in McNicholas, Murphy, McDaid & Frost (2010), we stop our EM algorithms when

$$l_\infty^{(k+1)} - l^{(k)} < \epsilon, \quad (16)$$

provided this difference is positive. The main benefit of this criterion when compared to lack of progress, is that the likelihood can sometimes “plateau” before increasing again. Accordingly, if lack of progress is used, the algorithm may terminate prematurely (see McNicholas, Murphy, McDaid & Frost 2010). However, the criterion in (16) helps overcome this problem by considering the likelihood after very many iterations, i.e., l_∞ .

3.4 A Note on Identifiability

It is important to note that, for each of the distributions discussed herein, the estimates for Σ_g and Ψ_g are only unique up to a strictly positive constant. Therefore, to eliminate the identifiability issue, a constraint needs to be imposed on Σ_g or Ψ_g . Anderlucci & Viroli (2015), suggest taking the trace of Ψ_g to be equal to p ; however, it is much simpler to set the first diagonal element of Σ_g to be 1 and this is the constraint we use in the analyses herein.

Discussion of identifiability would not be complete without mention of the label switching problem. This well-known problem is due to the invariance of the mixture model to relabelling of the components (Redner & Walker 1984, Stephens 2000). While the label switching problem is a real issue in the Bayesian paradigm (see Stephens 2000, Celeux, Hurn, & Robert 2000, for some discussion), it is of no practical concern for the work carried out herein. However, it is a theoretical identifiability issue and we note that it be resolved by specifying some ordering on the model parameters, e.g., simply requiring that $\pi_1 > \pi_2 > \dots > \pi_G$ often works and ordering on other parameters can be imposed as needed.

3.5 Number of Components and Performance Evaluation

In a general clustering scenario, the number of components (groups) G are not known *a priori*. It is, therefore, necessary to select an adequate number of components. There are two methods that are quite common in the literature. The first is the Bayesian information criterion (BIC; Schwarz 1978), which is defined as

$$\text{BIC} = 2\ell(\hat{\boldsymbol{\vartheta}}) - p \log N,$$

where $\ell(\hat{\boldsymbol{\vartheta}})$ is the maximized log-likelihood, N is the number of observations, and p is the number of free parameters. Another criterion common in the literature is the integrated completed likelihood (ICL; Biernacki, Celeux & Govaert 2000). The ICL can be approximated as

$$\text{ICL} \approx \text{BIC} + 2 \sum_{i=1}^N \sum_{g=1}^G \text{MAP}(\hat{z}_{ig}) \log \hat{z}_{ig},$$

where

$$\text{MAP}(\hat{z}_{ig}) = \begin{cases} 1 & \text{if } \arg \max_{h=1, \dots, G} \{\hat{z}_{ih}\} = g, \\ 0 & \text{otherwise.} \end{cases}$$

The ICL can be viewed as penalized version of the BIC, where the penalty is for uncertainty in the component membership.

To evaluate clustering performance, we consider the adjusted Rand index (ARI; Hubert & Arabie 1985). The ARI compares two different partitions, i.e., two different classifications in our applications. When the predicted classification is compared the actual classification, an ARI of 1 corresponds to perfect classification, whereas a value of 0 indicates the predicted classification is no better than randomly assigning the labels. Detailed review and discussion of the ARI is provided by Steinley (2004).

3.6 Semi-Supervised Classification

In addition to clustering (unsupervised classification), the matrix variate mixture models introduced here can also be applied for semi-supervised classification. Suppose that N matrices are observed but that we know the labels for K of the N matrices; specifically, suppose that K of the N matrices come from one of G classes. By analogy with McNicholas (2010), and without loss of generality, order these matrices so it is the first K that have known labels: $\mathbf{X}_1, \dots, \mathbf{X}_K, \mathbf{X}_{K+1}, \dots, \mathbf{X}_N$. Now, we know the values of z_{ig} for $i = 1, \dots, K$ and the observed-data likelihood is

$$L(\boldsymbol{\vartheta}) = \prod_{i=1}^K \prod_{g=1}^G [\pi_g f(\mathbf{X}_i \mid \mathbf{M}_g, \mathbf{A}_g, \boldsymbol{\Sigma}_g, \boldsymbol{\Psi}_g, \boldsymbol{\theta}_g)]^{z_{ig}} \times \prod_{j=K+1}^N \sum_{h=1}^H \pi_g f(\mathbf{X}_j \mid \mathbf{M}_h, \mathbf{A}_h, \boldsymbol{\Sigma}_h, \boldsymbol{\Psi}_h, \boldsymbol{\theta}_h),$$

where $\boldsymbol{\theta}_g$ are the parameters associated with the distribution of W_{ig} . In general, $H \geq G$; however, for the analyses herein, we make the common assumption that $H = G$. Parameter estimation, identifiability, etc., follow in an analogous fashion to the clustering case already described herein. Further details on semi-supervised classification in the mixture model setting are given in McLachlan & Peel (2000) and McNicholas (2016a).

4 Simulations

4.1 Overview

Two simulations are performed, where the first simulation has two groups and the second has three. The chosen parameters have no intrinsic meaning; however, they can be viewed as representations of multivariate longitudinal data and the parameters introduced by the distribution of W_{ig} are meant to illustrate the flexibility in concentration. Simulation 1 considers 3×4 data, Simulation 2 illustrates 4×3 data. In the first simulation, $\boldsymbol{\Sigma}_g$ and $\boldsymbol{\Psi}_g$

are set to

$$\begin{aligned}\Sigma_1 &= \begin{pmatrix} 1 & 0.5 & 0.1 \\ 0.5 & 1 & 0.5 \\ 0.1 & 0.5 & 1 \end{pmatrix}, & \Sigma_2 &= \begin{pmatrix} 1 & 0.1 & 0.1 \\ 0.1 & 1 & 0.1 \\ 0.1 & 0.1 & 1 \end{pmatrix}, \\ \Psi_1 &= \begin{pmatrix} 1 & 0.5 & 0.5 & 0.5 \\ 0.5 & 1 & 0 & 0 \\ 0.5 & 0 & 1 & 0 \\ 0.5 & 0 & 0 & 1 \end{pmatrix}, & \Psi_2 &= \begin{pmatrix} 1 & 0 & 0 & 0 \\ 0 & 1 & 0.5 & 0.5 \\ 0 & 0.5 & 1 & 0.2 \\ 0 & 0.5 & 0.2 & 1 \end{pmatrix}.\end{aligned}$$

For notational purposes, let $\tilde{\Sigma}_g$ and $\tilde{\Psi}_g$ be the scale matrices used in Simulation 2. We set $\tilde{\Sigma}_1 = \Psi_1$, $\tilde{\Sigma}_2 = \tilde{\Sigma}_3 = \Psi_2$ and $\tilde{\Psi}_1 = \tilde{\Psi}_3 = \Sigma_1$ and $\tilde{\Psi}_2 = \Sigma_2$. For each distribution, the models are fitted for $G \in \{1, 2, 3, 4\}$ and the BIC is used to choose the number of groups.

4.2 Simulation 1

In Simulation 1, for all four distributions, we take the location and skewness matrices to be:

$$\begin{aligned}\mathbf{M}_1 &= \begin{pmatrix} 1 & 0 & 0 & -1 \\ 0 & 1 & -1 & 0 \\ -1 & 0 & 2 & -1 \end{pmatrix}, & \mathbf{M}_2 &= \begin{pmatrix} 3 & 4 & 2 & 4 \\ 4 & 3 & 3 & 3 \\ 3 & 4 & 2 & 4 \end{pmatrix}, \\ \mathbf{A}_1 &= \begin{pmatrix} 1 & -1 & 0 & 1 \\ 1 & -1 & 0 & 1 \\ 1 & -1 & 0 & 1 \end{pmatrix}, & \mathbf{A}_2 &= \begin{pmatrix} 1 & 1 & 1 & -1 \\ 1 & 1 & 0.5 & -1 \\ 1 & 1 & 0 & -1 \end{pmatrix}.\end{aligned}$$

For the additional parameters, we took $\nu_1 = 4, \nu_2 = 20$ for the skew- t distribution, $\lambda_1 = \lambda_2 = 2$ and $\omega_1 = 4, \omega_2 = 2$ for the generalized hyperbolic distribution, $\gamma_1 = 7, \gamma_2 = 14$ for the variance-gamma distribution, and $\tilde{\gamma}_1 = 1/2, \tilde{\gamma}_2 = 2$ for the NIG distribution. Figure 1 in Appendix A shows a typical dataset for each distribution. For visualization, we look at the marginal columns which we label V1, V2, V3 and V4. We see that for all of the columns, except column 4, there is a clear separation between the two groups. We also note that for the skew- t distribution, there was a severe outlier in group 2 (due to the small degrees of freedom) that we do not show for better visualization. The orange dotted line is the marginal location parameter for the first group, and the yellow dotted line is the marginal location for the second group.

Table 1 displays the number of groups (components) chosen and the average ARI values with the associated standard deviations. The ICL results are identical, and thus are not shown here. We see that the correct number of groups is chosen, with perfect classification, for all 30 of the datasets when using the MVST, MVVG, and MVNIG mixtures. However, this is not the case with MVGH mixture, which underperforms when compared to the other three. However, the eight datasets for which the incorrect number of components is chosen correspond to datasets for which the two-component MVGH solution did not converge and, in a real application, alternative starting values would be pursued until convergence is achieved for the $G = 2$ component case.

Table 1: The number of groups chosen by the BIC and the average ARI values, with standard deviations in parentheses, for Simulation 1. Note that the MVGH mixture did not converge for eight of the 30 runs with $G = 2$.

	$G = 1$	$G = 2$	$G = 3$	$G = 4$	ARI (std. dev.)
MVST	0	30	0	0	1.00 (0.00)
MVGH	4	22	1	3	0.85 (0.34)
MVVG	0	30	0	0	1.00 (0.00)
MVNIG	0	30	0	0	1.00 (0.00)

In Table 2, we show the average amount of time per dataset to run the algorithm for $G = 1, 2, 3, 4$. We note that these simulations were performed in parallel.

Table 2: Average runtimes for Simulation 1.

Distribution	Average Time (s)
MVST	237.33
MVGH	625.90
MVVG	82.77
MVNIG	349.47

4.3 Simulation 2

In Simulation 2, a three group mixture was considered with 200 observations per group and the following location and skewness parameters.

$$\mathbf{M}_1 = \begin{pmatrix} 1 & -1 & 0 \\ 0 & 0 & -1 \\ 0 & 1 & 0 \\ -1 & 0 & -1 \end{pmatrix}, \quad \mathbf{M}_2 = \begin{pmatrix} -1 & 1 & 0 \\ 0 & 0 & 1 \\ 0 & -1 & 0 \\ 1 & 0 & 1 \end{pmatrix}, \quad \mathbf{M}_3 = \begin{pmatrix} 1 & 1 & 2 \\ 1 & 2 & 0 \\ 0 & 1 & 1 \\ 0 & 1 & 0 \end{pmatrix},$$

$$\mathbf{A}_1 = \begin{pmatrix} 1 & -1 & -1 \\ 1 & -0.5 & -1 \\ 1 & 0 & -1 \\ 1 & 0 & -1 \end{pmatrix}, \quad \mathbf{A}_2 = \mathbf{A}_3 = \begin{pmatrix} 1 & 1 & -1 \\ 1 & 0.5 & 0.5 \\ 1 & 0 & 0 \\ 1 & 0 & 0 \end{pmatrix}.$$

The other parameters we set to $\nu_1 = 4$, $\nu_2 = 8$, $\nu_3 = 20$ for the MVST, $\lambda_1 = 4$, $\lambda_2 = 0$, $\lambda_3 = -2$ and $\omega_1 = 4$, $\omega_2 = \omega_3 = 2$ for the MVGH, $\gamma_1 = 7$, $\gamma_2 = 9$, $\gamma_3 = 14$ for the MVVG and $\tilde{\gamma}_1 = 1/2$, $\tilde{\gamma}_2 = 1$, $\tilde{\gamma}_3 = 2$ for the MVNIG.

Again, the marginal distributions of a typical dataset is shown in Figure 2 in Appendix A. The dotted lines again represent the marginal locations, with orange for the first group, yellow for the second, and purple for the third. In Table 3, the number of groups chosen by

the BIC as well as the average ARI values, and associated standard deviations, are presented. As before, the MVST, MVVG and MVNIG mixtures outperform the MVGH mixture and, once again, this is due to convergence issues. The issue with convergence for the MVGH mixture with both simulations is possibly due to the update for, or impact of, the index parameters $\lambda_1, \dots, \lambda_G$.

Table 3: The number of groups chosen by the BIC and the average ARI values, with standard deviations in parentheses, for Simulation 2. Note that the MVGH mixture did not converge for 22 of the 30 runs with $G = 2$.

	$G = 1$	$G = 2$	$G = 3$	$G = 4$	ARI (std. dev.)
MVST	0	0	30	0	0.97 (0.010)
MVGH	10	8	8	4	0.52 (0.41)
MVVG	0	0	30	0	0.98 (0.0077)
MVNIG	0	0	30	0	0.99 (0.0056)

Table 4 shows the average runtime per dataset for Simulation 2. Notice that for the MVGH, MVVG and MVNIG mixtures, each dataset took longer on average, with the MVGH mixture having the longest runtime as well as the largest increase in runtime over Simulation 1. This is to be expected because there is an increase in the number of groups and observations; however, for the MVVG and MVNIG mixtures, the time differences between Simulations 1 and 2 are less notable. The MVST mixture actually took less time on average; however, this is because a few datasets for Simulation 1 ran to the maximum number of iterations (without converging) for the $G = 4$ group mixture thus increasing the runtime.

Table 4: Average runtimes for Simulation 2.

Distribution	Average Time (s)
MVST	233.67
MVGH	2542.50
MVVG	171.90
MVNIG	581.63

5 Image Recognition Example

We now apply the matrix variate mixture models introduced herein to image recognition with the MNIST handwriting dataset (LeCun, Bottou, Bengio & Haffner 1998). The original dataset consists of 60,000 training images of handwritten digits 0 to 9, which can be represented as 28×28 pixel matrices with greyscale intensities ranging from 0 to 255. However, these dimensions resulted in an infinite calculation for the Bessel function and its derivative with respect to λ . Moreover, because two unstructured 28×28 dimensional covariance

matrices would need to be estimated, model fitting would be infeasible. We stress that this alone is an indication that dimension reduction techniques will need to be developed in the future. However, the main goal of this application is to demonstrate the discussed methods outside of the theoretical confines of the simulations. Therefore, we resized the original image to a 10×10 pixel matrix using the *resize* function in the **EImage** package (Pau, Fuchs, Sklyar, Boutros & Huber 2010) for the R software (R Core Team 2016). However, there are problems with sparsity. Specifically, the outside columns and rows all contain values of 0 because they are outside of the main writing space. Accordingly, there is no variation in these outer columns and rows, therefore resulting in exactly singular Σ_g and Ψ_g updates. To solve this problem, we replace a value of 0 with a value between 0 and 2 with increments of 0.1 and added 50 to the non-zero values to make sure the noise did not interfere with the true signal.

Each of the matrix variate mixtures introduced herein is applied within the semi-supervised classification paradigm (Section 3.6). A total of 500 observations from digit 1 and 500 from digit 7 are sampled from the training set, and then 100 of each of these digits is considered unlabelled, i.e., 80% of the data are labelled. We performed the analysis on 30 different such sets. In Table 5, we show aggregate classification tables for the points considered unlabelled for each of the matrix variate mixtures. In Table 6, we show the average ARI values and the average misclassification rates for the unlabelled points. Note, that for some of the datasets, not all four mixtures converged; therefore, the total number of observations in the tables need not be the same for all four distributions. Looking at the classification tables, it is clear that all of these matrix variate mixtures overall misclassify digit 1 as digit 7 more often than digit 7 as digit 1. From both the ARI and MCR results, the MVVG mixture slightly outperforms the other three mixtures. It is interesting to note that the MVGH mixture did not experience the same convergence issues as seen with the simulations. This is almost certainly because 80% of the data points have known labels here whereas, in the simulations, we used the clustering (unsupervised classification) scenario and so all of the labels are unknown.

Table 5: Cross-tabulations of true (1,7) versus predicted (P1, P7) classifications for the points considered unlabelled in the MNIST data, for each of the matrix variate mixtures introduced herein, aggregated over all runs (for which convergence was attained).

MVST			MVGH		MVVG		MVNIG	
	P1	P7	P1	P7	P1	P7	P1	P7
1	2797	203	2813	187	2859	141	2798	202
7	127	2873	125	2875	122	2878	127	2873

6 Discussion

Four matrix variate mixture distributions, with component densities that parameterize skewness, have been used for model-based clustering — and its semi-supervised analogue — of

Table 6: Average ARI values and misclassification rates (MCR), with associated standard deviations in parentheses, for each matrix variate mixture approach for the points considered unlabelled for the MNIST data, aggregated over all runs (for which convergence was attained).

	ARI (std. dev.)	MCR (std. dev.)
MVST	0.79 (0.051)	0.055 (0.014)
MVGH	0.80 (0.056)	0.052 (0.016)
MVVG	0.83 (0.043)	0.044 (0.012)
MVNIG	0.79 (0.051)	0.055 (0.014)

three-way data. Specifically, we considered MVST, MVGH, MVVG, and MVNIG mixtures, respectively, and an ECM algorithm was used for parameter estimation in each case. Simulated and real data were used for illustration. In the first simulation, there was good separation between the two groups and, in the second, we increased the number of groups, decreased the separation between the groups, and obtained similar results to the first. In both simulations, the MVGH mixture often underperformed when compared to the other three mixtures due to convergence issues. This could be resolved, for example, by restricting the index parameter λ ; however, doing this would essentially eliminate the additional flexibility enjoyed by the MVGH mixture. In the real data application, the MVVG mixture outperformed the other three mixtures in terms of both average ARI and average misclassification rate, and the MVVG mixture consistently ran faster than the other three mixtures.

The next step in this work is to introduce parsimony into the matrix variate mixture models introduced herein. A very simple way to introduce parsimony is to take the eigenvalue decomposition of the scale matrices to form a family of parsimonious mixture models, along similar lines to (Celeux & Govaert 1995). Another important area, though slightly more difficult, is dimension reduction. Recall, in the MNIST data application, that the original data had to be resized due to problems evaluating the Bessel function as well as feasibility issues. One possible solution is to consider a matrix variate analogue of the mixture of factor analyzers model (Ghahramani & Hinton 1997) and this will be a topic of future work. Another possibility for future work is the application of these models to multivariate longitudinal data (e.g., as in Anderlucci & Viroli 2015), in which case it would be important to impose a structure on Σ_g . Finally, the unsupervised and semi-supervised classification paradigms have been investigated herein but some future work will focus on applying these matrix variate mixtures within the fractionally-supervised classification framework (Vrbik & McNicholas 2015, Gallagher & McNicholas 2017c).

Acknowledgements

The authors gratefully acknowledge the support of a Vanier Canada Graduate Scholarship (Gallagher) and the Canada Research Chairs program (McNicholas).

References

- Aitken, A. C. (1926), ‘A series formula for the roots of algebraic and transcendental equations’, *Proceedings of the Royal Society of Edinburgh* **45**, 14–22.
- Anderlucci, L. & Viroli, C. (2015), ‘Covariance pattern mixture models for the analysis of multivariate heterogeneous longitudinal data’, *The Annals of Applied Statistics* **9**(2), 777–800.
- Andrews, J. L. & McNicholas, P. D. (2011), ‘Extending mixtures of multivariate t-factor analyzers’, *Statistics and Computing* **21**(3), 361–373.
- Andrews, J. L. & McNicholas, P. D. (2012), ‘Model-based clustering, classification, and discriminant analysis via mixtures of multivariate t -distributions: The t EIGEN family’, *Statistics and Computing* **22**(5), 1021–1029.
- Baricz, A. (2010), ‘Turn type inequalities for some probability density functions’, *Studia Scientiarum Mathematicarum Hungarica* **47**, 175–189.
- Baum, L. E., Petrie, T., Soules, G. & Weiss, N. (1970), ‘A maximization technique occurring in the statistical analysis of probabilistic functions of Markov chains’, *Annals of Mathematical Statistics* **41**, 164–171.
- Biernacki, C., Celeux, G. & Govaert, G. (2000), ‘Assessing a mixture model for clustering with the integrated completed likelihood’, *IEEE Transactions on Pattern Analysis and Machine Intelligence* **22**(7), 719–725.
- Biernacki, C., Celeux, G. & Govaert, G. (2003), ‘Choosing starting values for the EM algorithm for getting the highest likelihood in multivariate Gaussian mixture models’, *Computational Statistics and Data Analysis* **41**, 561–575.
- Böhning, D., Dietz, E., Schaub, R., Schlattmann, P. & Lindsay, B. (1994), ‘The distribution of the likelihood ratio for mixtures of densities from the one-parameter exponential family’, *Annals of the Institute of Statistical Mathematics* **46**, 373–388.
- Bouguila, N. & ElGuebaly, W. (2009), ‘Discrete data clustering using finite mixture models’, *Pattern Recognition* **42**(1), 33–42.
- Browne, R. P. & McNicholas, P. D. (2015), ‘A mixture of generalized hyperbolic distributions’, *Canadian Journal of Statistics* **43**(2), 176–198.
- Celeux, G. & Govaert, G. (1995), ‘Gaussian parsimonious clustering models’, *Pattern Recognition* **28**(5), 781–793.
- Celeux, G., Hurn, M., & Robert, C. P. (2000), ‘Computational and inferential difficulties with mixture posterior distributions’, *Journal of the American Statistical Association* **95**, 957–970.
- Chen, J. T. & Gupta, A. K. (2005), ‘Matrix variate skew normal distributions’, *Statistics* **39**(3), 247–253.
- Dang, U. J., Browne, R. P. & McNicholas, P. D. (2015), ‘Mixtures of multivariate power exponential distributions’, *Biometrics* **71**(4), 1081–1089.

- Doğru, F. Z., Bulut, Y. M. & Arslan, O. (2016), ‘Finite mixtures of matrix variate t distributions’, *Gazi University Journal of Science* **29**(2), 335–341.
- Domínguez-Molina, J. A., González-Farías, G., Ramos-Quiroga, R. & Gupta, A. K. (2007), ‘A matrix variate closed skew-normal distribution with applications to stochastic frontier analysis’, *Communications in Statistics–Theory and Methods* **36**(9), 1691–1703.
- Elguebaly, T. & Bouguila, N. (2015), ‘Simultaneous high-dimensional clustering and feature selection using asymmetric Gaussian mixture models’, *Image and Vision Computing* **34**(6), 27–41.
- Franczak, B. C., Browne, R. P. & McNicholas, P. D. (2014), ‘Mixtures of shifted asymmetric Laplace distributions’, *IEEE Transactions on Pattern Analysis and Machine Intelligence* **36**(6), 1149–1157.
- Franczak, B. C., Tortora, C., Browne, R. P. & McNicholas, P. D. (2015), ‘Unsupervised learning via mixtures of skewed distributions with hypercube contours’, *Pattern Recognition Letters* **58**(1), 69–76.
- Gallaughar, M. P. B. & McNicholas, P. D. (2017a), ‘A matrix variate skew-t distribution’, *Stat* **6**(1), 160–170.
- Gallaughar, M. P. B. & McNicholas, P. D. (2017b), ‘Three skewed matrix variate distributions’, arXiv preprint arXiv:1704.02531.
- Gallaughar, M. P. B. & McNicholas, P. D. (2017c), ‘On fractionally-supervised classification: Weight selection and extension to the multivariate t-distribution’, arXiv preprint arXiv:1709.08258.
- Ghahramani, Z. & Hinton, G. E. (1997), The EM algorithm for factor analyzers. Technical Report CRG-TR-96-1, University of Toronto, Toronto, Canada.
- Gupta, A. K. & Nagar, D. K. (1999), *Matrix Variate Distributions*, Chapman & Hall/CRC Press, Boca Raton.
- Harrar, S. W. & Gupta, A. K. (2008), ‘On matrix variate skew-normal distributions’, *Statistics* **42**(2), 179–194.
- Hubert, L. & Arabie, P. (1985), ‘Comparing partitions’, *Journal of Classification* **2**(1), 193–218.
- Karlis, D. & Meligkotsidou, L. (2007), ‘Finite mixtures of multivariate Poisson distributions with application’, *Journal of Statistical Planning and Inference* **137**, 1942–1960.
- Karlis, D. & Santourian, A. (2009), ‘Model-based clustering with non-elliptically contoured distributions’, *Statistics and Computing* **19**(1), 73–83.
- LeCun, Y., Bottou, L., Bengio, Y. & Haffner, P. (1998), ‘Gradient-based learning applied to document recognition’, *Proceedings of the IEEE* **86**(11), 2278–2324.
- Lee, S. & McLachlan, G. J. (2014), ‘Finite mixtures of multivariate skew t-distributions: some recent and new results’, *Statistics and Computing* **24**(2), 181–202.
- Lee, S. X. & McLachlan, G. J. (2016), ‘Finite mixtures of canonical fundamental skew t-distributions’, *Statistics and Computing* **26**(3), 573–589.

- Lin, T.-I. (2010), ‘Robust mixture modeling using multivariate skew t distributions’, *Statistics and Computing* **20**(3), 343–356.
- Lin, T.-I., McNicholas, P. D. & Hsiu, J. H. (2014), ‘Capturing patterns via parsimonious t mixture models’, *Statistics and Probability Letters* **88**, 80–87.
- Lindsay, B. G. (1995), Mixture models: Theory, geometry and applications, in ‘NSF-CBMS Regional Conference Series in Probability and Statistics’, Vol. 5, Hayward, California: Institute of Mathematical Statistics.
- McLachlan, G. and Peel, D. (2000), *Finite Mixture Models*, John Wiley & Sons, New York.
- McNicholas, P. D. (2010), ‘Model-based classification using latent Gaussian mixture models’, *Journal of Statistical Planning and Inference* **140**(5), 1175–1181.
- McNicholas, P. D. (2016a), *Mixture Model-Based Classification*, Chapman & Hall/CRC Press, Boca Raton.
- McNicholas, P. D. (2016b), ‘Model-based clustering’, *Journal of Classification* **33**(3), 331–373.
- McNicholas, P. D., Murphy, T. B., McDaid, A. F. & Frost, D. (2010), ‘Serial and parallel implementations of model-based clustering via parsimonious Gaussian mixture models’, *Computational Statistics and Data Analysis* **54**(3), 711–723.
- McNicholas, S. M., McNicholas, P. D. & Browne, R. P. (2017), A mixture of variance-gamma factor analyzers in Ahmed, S. E. (ed.), ‘Big and Complex Data Analysis: Methodologies and Applications’, pp. 369–385. Springer International Publishing, Cham, Switzerland.
- Meng, X.-L. & Rubin, D. B. (1993), ‘Maximum likelihood estimation via the ECM algorithm: a general framework’, *Biometrika* **80**, 267–278.
- Morris, K. & McNicholas, P. D. (2013), ‘Dimension reduction for model-based clustering via mixtures of shifted asymmetric Laplace distributions’, *Statistics and Probability Letters* **83**(9), 2088–2093.
- Murray, P. M., Browne, R. P. & McNicholas, P. D. (2014), ‘Mixtures of skew-t factor analyzers’, *Computational Statistics and Data Analysis* **77**, 326–335.
- Murray, P. M., Browne, R. P. & McNicholas, P. D. (2017), ‘Hidden truncation hyperbolic distributions, finite mixtures thereof, and their application for clustering’, *Journal of Multivariate Analysis* **161**, 141–156.
- Murray, P. M., McNicholas, P. D. & Browne, R. P. (2014), ‘A mixtures of common skew-t factor analyzers’, *Stat* **3**(1), 68–82.
- Pau, G., Fuchs, F., Sklyar, O., Boutros, M. & Huber, W. (2010), ‘Ebimage—an R package for image processing with applications to cellular phenotypes’, *Bioinformatics* **26**(7), 979–981.
- Peel, D. & McLachlan, G. J. (2000), ‘Robust mixture modelling using the t distribution’, *Statistics and Computing* **10**(4), 339–348.
- R Core Team (2016), R: A Language and Environment for Statistical Computing. Vienna, Austria: R Foundation for Statistical Computing.

- Redner, R. A. and H. F. Walker (1984), ‘Mixture densities, maximum likelihood and the EM algorithm’, *SIAM Review* **26**, 195–239.
- Schwarz, G. (1978), ‘Estimating the dimension of a model’, *The Annals of Statistics* **6**(2), 461–464.
- Scott, A. J. & Symons, M. J. (1971), ‘Clustering methods based on likelihood ratio criteria’, *Biometrics* **27**, 387–397.
- Steinley, D. (2004), ‘Properties of the Hubert-Arabie adjusted Rand index’, *Psychological Methods* **9**, 386–396.
- Stephens, M. (2000), ‘Dealing with label switching in mixture models’, *Journal of Royal Statistical Society: Series B* **62**, 795–809.
- Subedi, S. and McNicholas, P. D. (2014), ‘Variational Bayes approximations for clustering via mixtures of normal inverse Gaussian distributions’, *Advances in Data Analysis and Classification* **8**(2), 167–193.
- Tiedeman, D. V. (1955), On the study of types, in S. B. Sells, ed., ‘Symposium on Pattern Analysis’, Air University, U.S.A.F. School of Aviation Medicine, Randolph Field, Texas.
- Viroli, C. (2011), ‘Finite mixtures of matrix normal distributions for classifying three-way data’, *Statistics and Computing* **21**(4), 511–522.
- Vrbik, I. & McNicholas, P. D. (2012), ‘Analytic calculations for the EM algorithm for multivariate skew-t mixture models’, *Statistics and Probability Letters* **82**(6), 1169–1174.
- Vrbik, I. & McNicholas, P. D. (2014), ‘Parsimonious skew mixture models for model-based clustering and classification’, *Computational Statistics and Data Analysis* **71**, 196–210.
- Vrbik, I. & McNicholas, P. D. (2015), ‘Fractionally-supervised classification’, *Journal of Classification* **32**(3), 359–381.
- Wishart, J. (1928), ‘The generalised product moment distribution in samples from a normal multivariate population’, *Biometrika* **20A**(1–2), 32–52.
- Wolfe, J. H. (1965), A computer program for the maximum likelihood analysis of types, Technical Bulletin 65-15, U.S. Naval Personnel Research Activity.

A Figures

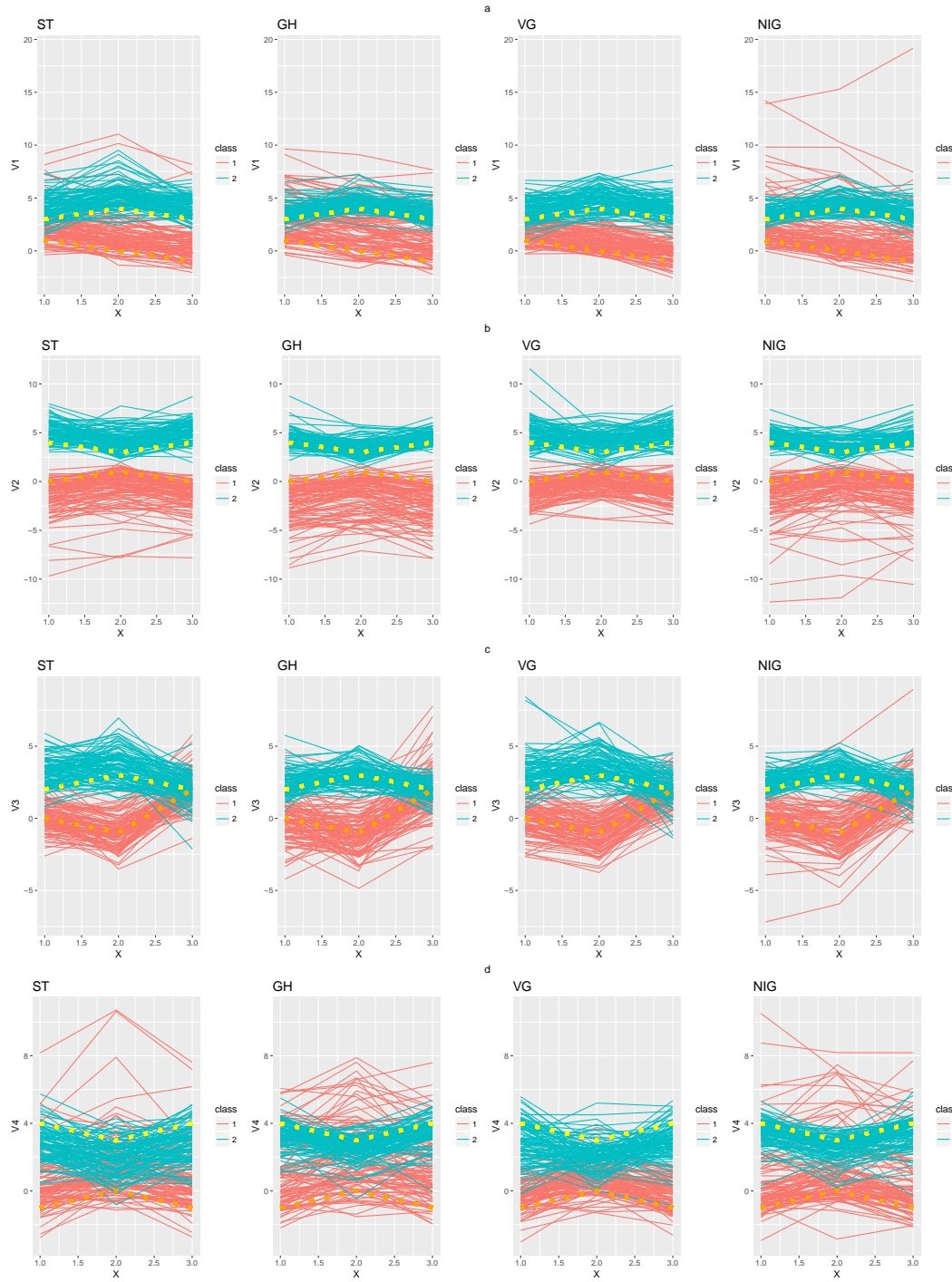


Figure 1: Marginal data for the columns for each of the four distributions for Simulation 1. The dotted lines represent the marginal location parameters with the orange as the marginal location for group 1 and the yellow for group 2.

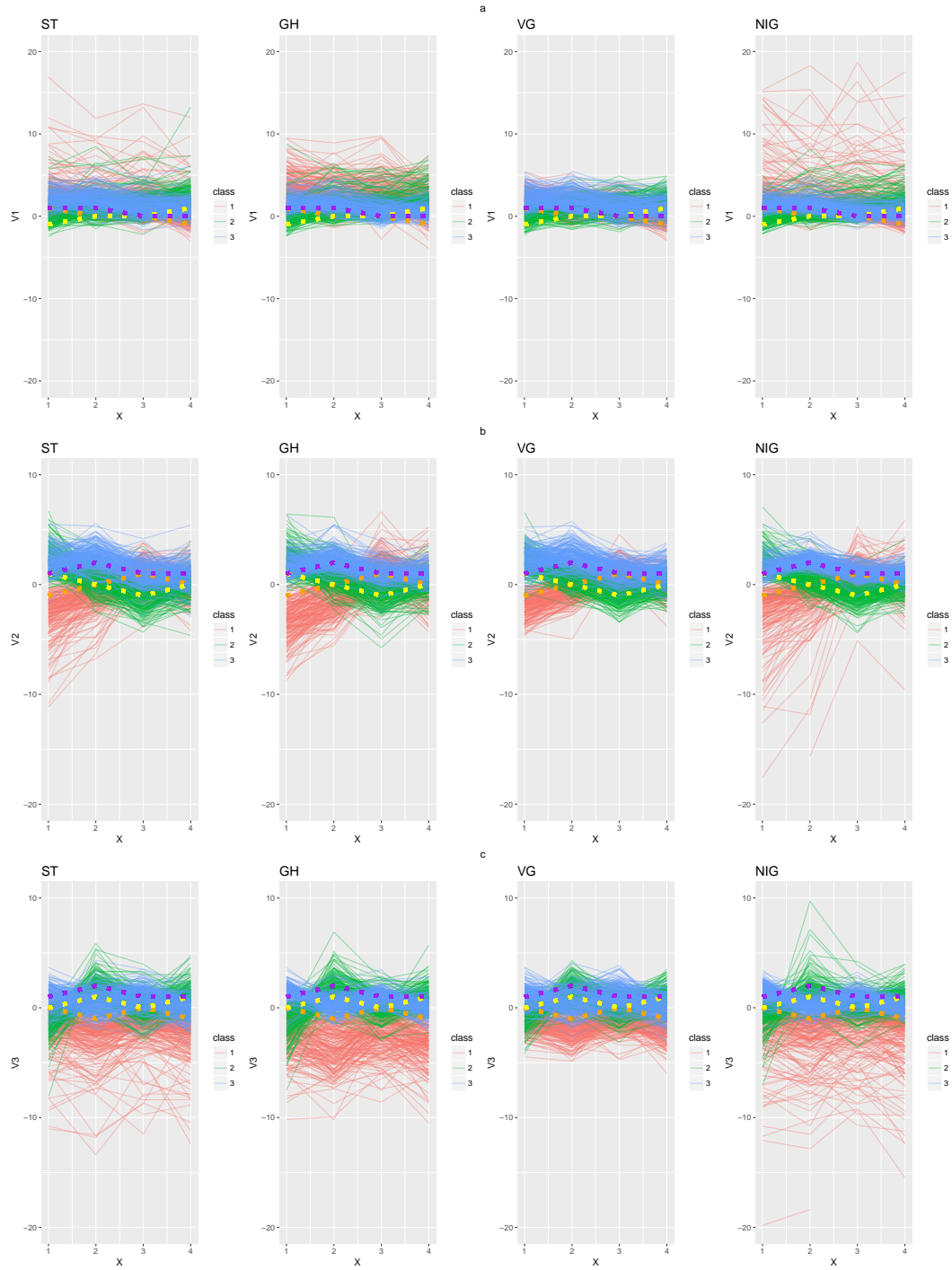


Figure 2: Marginal data for the columns for each of the four distributions for Simulation 2. The dotted lines represent the marginal location parameters with the orange as the marginal location for group 1, yellow for group 2, and purple for group 3.